ELSEVIER

Chemical Engineering Journal 77 (2000) 179–187

Chemical Engineering Journal

www.elsevier.com/locate/cej

Vapor–liquid equilibria of multi-indexed continuous mixtures using an equation of state and group contribution methods

F.C. Peixoto[a,b,1], G.M. Platt[b], F.L.P. Pessôa[b,*]

[a] *Instituto de Pesquisa e Desenvolvimento (IPD-CTEx), Av. das Américas 28705, Barra de Guaratiba, Rio de Janeiro, RJ, CEP: 23020-470, Brazil*

[b] *Depto. de Engenharia Química, Escola de Química, Univ. Federal do Rio de Janeiro, Centro de Tecnologia, Bloco E, Cidade Universitária, Caixa Postal: 68542, Rio de Janeiro, RJ, CEP: 21949-900, Brazil*

Received 13 March 1999; received in revised form 6 October 1999; accepted 26 November 1999

Abstract

In this work, vapor–liquid equilibria (VLE) calculations for a continuous mixture are carried out. The Peng–Robinson EOS is employed, and a new approach for parameter evaluation is proposed, using group contribution methods. This approach was possible through the use of a convenient choice for the characteristic continuous index. Multi-indexed continuous mixtures are focused on, which has been avoided in the literature probably because of the mathematical complexity of such modeling. Two algorithms were proposed for VLE calculations (flash with P and T fixed, bubble and dew points) and three kinds of continuous mixtures (linear paraffins, polyunsaturated fatty acids (PUFA) and oil fractions) were analyzed.

Keywords: Multi-indexed continuous mixtures; Vapor–liquid equilibria; Flash calculation; Quadrature method

1. Introduction

The concept of continuity of a given mixture is applied whenever that mixture is so complex that it is no longer worthwhile to distinguish among individual chemical species; instead, an index (such as number of carbon atoms, boiling point or chromatographic retention time) is chosen to characterize each component and the continuity of the index is assumed. Mole fraction x_i of species A_i is replaced by $f(x)\mathrm{d}x$, the molar fraction of material with an index in the $(x, x+\mathrm{d}x)$ interval. Function $f(x)$ is known as the mixture distribution function (DF), where x is the continuous index of the mixture.

In some cases, more than one index must be used to completely characterize the continuum of species, which increases the mathematical complexity of any phenomena described with a continuous approach. If $\underline{x}$ is a vector of continuous indices, the DF of the system is denoted by $f(\underline{x})$ and the molar fraction of species with indices in the region $(\underline{x}, \underline{x}+\mathrm{d}\underline{x})$ is given by the analogous expression $f(\underline{x})\mathrm{d}^n x$.

Distribution functions exhibit an obvious normalization condition given by

$$\int_0^\infty \cdots \int_0^\infty f(\underline{x})\mathrm{d}^n x = 1 \tag{1}$$

Vapor–liquid equilibria (VLE) calculations for complex mixtures have been traditionally accessed through a Pseudo-Component Method, that is basically a 'lumping' approach in which key components are chosen to fully characterize the whole mixture. This way, a simple modeling procedure can be adopted, but results are highly dependent on the choice of the set of pseudo-components [1]. The development of a continuous thermodynamics [2–5] had shown great advantages in many aspects [6–10].

However, the use of multivariate DFs has been avoided probably because of the already mentioned mathematical complexity. Systems that clearly needed more than one index have then been approximated by more than one family of species:

$$f(\underline{x}) \rightarrow f_i(x_i) \tag{2}$$

Another critical point is the choice of the continuous index. Some authors chose a natural identification variable, such as molecular weight or boiling point [6,7]. However, it is sometimes difficult to relate such indices with other thermodynamic properties, especially equations of state (EOS) parameters, and fitted polynomials have been employed [9].

This work aims at the modeling of VLE for continuous mixtures that are naturally characterized by multivari-

* Corresponding author. Tel.: +55-21-590-3192.
E-mail addresses: fpeixoto@ipd.eb.mil.br (F.C. Peixoto), gustavo-@compuland.com.br (G.M. Platt), pessoa@h2o.eq.ufrj.br (F.L.P. Pessôa).
[1] Tel.: +55-21-410-6288.

1385-8947/00/$ – see front matter
PII: S1385-8947(99)00161-8

ate DFs, the most important examples being petroleum fractions. The well-established Quadrature Method [7] is employed for solving flash problem (at fixed T and P) and bubble and dew point problems for such mixtures. This method was considered the most suitable, once it does not show the error in material balance of the Method of Moments [7]. EOS parameters are estimated through group contribution methods instead of the traditional fitted polynomials. This was possible admitting that the number of particular groups was the vector of continuous indices itself, which is also an original contribution of the present work.

2. Continuous thermodynamics for a multi-indexed mixture

As mentioned in Cotterman et al. [9], the fugacity coefficient is calculated as

$$RT\ln[\phi(\underline{x})] = \int_v^\infty \left\{ \left(\frac{\delta P}{\delta f(\underline{x}')} \right)_{T,v,\underline{x}'=\underline{x}} - \frac{RT}{v} \right\} \mathrm{d}v - RT\ln(z) \quad (3)$$

where δ stands for the functional derivative of the EOS with respect to the DF.

The present work uses Peng–Robinson cubic EOS [11] to describe both liquid and vapor phases:

$$P = \frac{RT}{v-b} - \frac{a}{(v+\delta_1 b)(v+\delta_2 b)} \quad (4)$$

with the parameters for the continuum of species defined by

$$a(\underline{x},T) = \Omega_a R^2 \frac{[T_c(\underline{x})]^2}{P_c(\underline{x})} \left\{ 1 + m[\omega(\underline{x})] \left[1 - \left(\frac{T}{T_c(\underline{x})} \right)^{1/2} \right] \right\}^2 \quad (5)$$

$$b(\underline{x}) = \Omega_b R \frac{T_c(\underline{x})}{P_c(\underline{x})} \quad (6)$$

where

$$m[\omega(\underline{x})] = r_0 + r_1\omega(\underline{x}) + r_2\omega(\underline{x})^2 \quad (7)$$

Mixing rules are written as

$$b = \int_0^\infty \cdots \int_0^\infty f(\underline{x}) b(\underline{x}) \mathrm{d}^n x \quad (8)$$

$$a(T) = \left[\int_0^\infty \cdots \int_0^\infty f(\underline{x}) \sqrt{a(\underline{x},T)} \mathrm{d}^n x \right]^2 \quad (9)$$

When the functional derivatives in Eq. (3) are conducted using expressions (4)–(9), Eq. (3) becomes (after integration)

$$\ln[\phi(\underline{x})] = \frac{b(\underline{x})}{b}(z-1) - \ln(z-B) - \frac{a(T)}{(\delta_1-\delta_2)bRT} \times \ln\left[\frac{v+\delta_1 b}{v+\delta_2 b} \right] \left[2\frac{a'(\underline{x},T)}{a(T)} - \frac{b(\underline{x})}{b} \right] \quad (10)$$

Table 1
Parameters of Peng–Robinson EOS

δ_1	$1+\sqrt{2}$
δ_3	$1-\sqrt{2}$
Ω_a	0.45724
Ω_b	0.07780
r_0	0.37464
r_1	1.54226
r_2	−0.26992

with the compressibility factor defined as usual:

$$z = \frac{Pv}{RT} \quad (11)$$

and additional entities by

$$a'(\underline{x},T) = \sqrt{a(\underline{x},T)} \int_0^\infty \cdots \int_0^\infty f(\underline{x}) \sqrt{a(\underline{x},T)} \mathrm{d}^n x \quad (12)$$

$$B = \frac{Pb}{RT} \quad (13)$$

Peng–Robinson EOS parameters can be found in Table 1.

Depending on the number of continuous indices, some particular aspects must be taken into account, which will be analyzed in the following sections. However, it will always be used a product of gamma distribution functions for the DF of feed or initial mixture:

$$f(\underline{x}) = \prod_{i=1}^n \frac{\varepsilon_i^{\eta_i+1} x_i^{\eta_i} \exp(-\varepsilon_i x_i)}{\Gamma(\eta_i+1)} = \prod_{i=1}^n f(x_i, \varepsilon_i, \eta_i) \quad (14)$$

This DF obeys the normalization constrain Eq. (1) and is able to emulate a discrete case where a single molecule is present:

$$\lim_{\substack{\eta_1,\varepsilon_1\to\infty \\ \eta_1/\varepsilon_1=d_1}} \cdots \lim_{\substack{\eta_n,\varepsilon_n\to\infty \\ \eta_n/\varepsilon_n=d_n}} f(\underline{x}) = \prod_{i=1}^n \delta(x_n - d_n) \quad (15)$$

3. Group contribution methods

Models for $a(\underline{x}, T)$ and $b(\underline{x})$ have been traditionally accessed through fitted polynomials [1,6,7,9,12] instead of their natural formulations given by Eqs. (5) and (6). As it can be seen, these equations demand a method to predict molecular properties (critical coordinates, for instance) as functions of the continuous vector parameter $\underline{x}$.

This can be carried out with well-established group contribution methods, as Joback [13] predictions for the acentric factor, normal boiling point and critical coordinates. If $\underline{x}$ is the number of groups in the molecular structure, the expressions are

$$\omega(\underline{x}) = \frac{3}{7} \frac{T_b(\underline{x})/T_c(\underline{x})}{1 - T_b(\underline{x})/T_c(\underline{x})} \log[P_c(\underline{x})] - 1 \quad (16)$$

$$T_b(\underline{x}) = 198 + \sum \Delta T_b(\underline{x}) \quad (17)$$

$$T_c(\underline{x}) = T_b(\underline{x})\left[0.584 + 0.965\sum \Delta T_c(\underline{x}) - \left(\sum \Delta T_c(\underline{x})\right)^2\right]^{-1} \quad (18)$$

$$P_c(\underline{x}) = \left[0.113 + 0.0032\mathrm{Na} - \sum \Delta P_c(\underline{x})\right]^{-2} \quad (19)$$

where Na stands for the total number of atoms in a molecule. All summations are performed over the groups present on the molecule, accounting individual contributions of each of these increments.

For vapor pressure prediction, the following group contribution method is employed [13]:

$$P^{sat}(\underline{x}, T) = \exp\left\{\frac{T_b(\underline{x})/T_c(\underline{x})}{1 - T_b(\underline{x})/T_c(\underline{x})}\left[1 - \left(\frac{T_c(\underline{x})}{T}\right)\right]\log[P_c(\underline{x})]\right\} \quad (20)$$

3.1. Case 1: single-indexed mixture — linear alkanes

An illustrative example for the single index case is a continuous mixture of linear alkanes. Its utility lies in the fact that it is a common strategy for some particular applications in petroleum processing theory, to study the behavior of oil as constituted basically by linear paraffinic molecules. A typical molecule is then completely characterized by the total atoms of carbon present in it (x) and Joback's vector for this case is then given by

$$\underline{J}(x) = \begin{bmatrix} -CH_2- \\ -CH_3 \end{bmatrix} = \begin{bmatrix} x-2 \\ 2 \end{bmatrix} \quad (21)$$

and individual contributions by the values in Table 2 (which has also additional group contributions that will be used in Cases 2 and 3).Summations in Eqs. (17), (19) and (20) are then performed as follows:

$$\sum \Delta T_c(x) = \underline{J}^t(x)\underline{\Delta} T_c(x) = 2(0.0141) + (x-2)0.0189 \quad (22)$$

$$\sum \Delta P_c(x) = \underline{J}^t(x)\underline{\Delta} P_c(x) = 2(-0.0012) \quad (23)$$

Table 2
Group contributions

Increments	ΔT_c	ΔP_c	ΔT_b
$-CH_2-$	0.0189	0	22.88
$-CH_3$	0.0141	−0.0012	23.58
–CH=	0.0129	−0.0006	24.96
–COOH	0.0791	0.0077	169.09
$> CH_2^r$	0.0100	0.0025	27.15
$>CH-^r$	0.0122	0.0004	21.78
$=CH-^r$	0.0082	0.0011	26.73
$>C=^r$	0.0143	0.0008	31.01

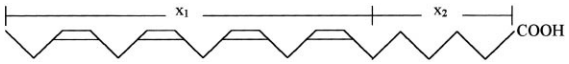

Fig. 1. PUFA.

$$\sum \Delta T_b(x) = \underline{J}^t(x)\underline{\Delta} T_b(x) = 2(23.58) + (x-2)22.88 \quad (24)$$

3.2. Case 2: double-indexed mixture — PUFA

For this case is employed a mixture of polyunsaturated fatty acids (PUFA). These mixtures are important because the human body is unable to synthesize them and relies on dietary intake for supply. This dietary supply could be vegetable oil, but the mixture present in fish oil exhibits higher health benefits. Some of its components decrease the danger of premature birth and a separation procedure would be of great interest. Of course, there is the problem of thermosensitivity; and supercritical extraction with CO_2 would be the preferred operation. However, it is obviously useful to have knowledge on volatility and other VLE information.

A typical molecule of this mixture is depicted in Fig. 1 where it can be seen that an index corresponds to the number of carbon atoms in the unsaturated part of the molecule and the other to the saturated one.

Summations for this case are completely analogous to the ones described in Eqs. (22)–(24), and employ a Joback vector with the form

$$\underline{J}(\underline{x}) = \begin{bmatrix} -CH= \\ -CH_2- \\ -CH_3 \\ -COOH \end{bmatrix} = \begin{bmatrix} 2(x_1-2)/3 \\ (x_1+1)/3 + x_2 \\ 1 \\ 1 \end{bmatrix} \quad (25)$$

and values of Table 2.

3.3. Case 3: three-indexed mixture — oil fractions

Mixtures chosen to be characterized by three-indexed continua were typical petroleum fractions, such as gasoil, gasoline or naphtha. Once species present in gasoil ranged from simple linear alkanes to very complex molecules with distributed aromatic and naphthenic rings over its structure, an arbitrarily structural description for typical molecules was defined. An elementary model for a continuous species representation was established, based on the conclusions of Quann and Jaffe [14] about the most common patterns of molecular structures present in petroleum:

1. Paraffinic compounds and paraffinic portions present in multifunctional compounds are mainly linear.
2. Ring compounds are mainly cata-condensed, which means that, at each pair of rings, an 'ascending' displacement is observed, in the aromatic region (Fig. 2); and in the naphthenic region (Fig. 3).
3. Multifunctional compounds show a single paraffinic ramification.

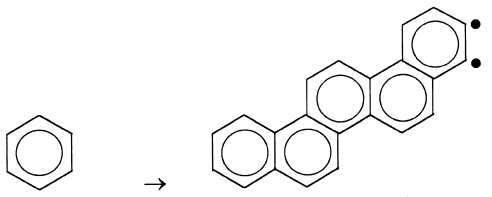

Fig. 2. Cata-condensation of aromatic rings.

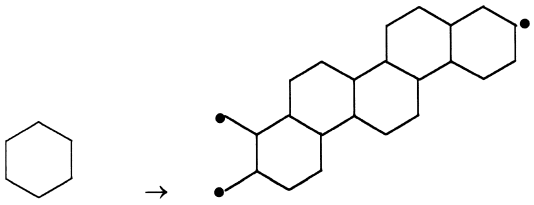

Fig. 3. Cata-condensation of naphthenic rings.

Even though other configurations may be found in petroleum fractions (isoalkanes and other kinds of juxtaposition of naphthenic and/or aromatic rings), we opted for the simplest way to access the maximum number of molecular properties with the minimum number of continuous indices. For that, the conclusions of Quann and Jaffe [14] seemed to be the most adequate, and they state that isomers of a molecular class, at a given carbon number, exhibit similar physical, chemical, thermodynamic, and performance properties, since this is the limit of our analytical detail, which minimizes the effect of not considering such isomers.

As already mentioned, the present representation is based on admitting three types of sub-structures continuously present in each species: aromatic sub-structure, naphthenic sub-structure and paraffinic sub-structure. Each of these sub-structures will be henceforth characterized by a non-negative continuous index. The connectivity among these sub-structures will be arbitrarily set as given in Fig. 4 also admitting the absence of side paraffinic ramifications.

With all these considerations, Joback vector becomes

$$\underline{J}(\underline{x}) = \begin{bmatrix} \text{–CH}_3 \\ \text{–CH}_2\text{–} \\ \text{=CH–}^{\text{r}} \\ > \text{CH}_2^{\text{r}} \\ > \text{C=}^{\text{r}} \\ > \text{CH–}^{\text{r}} \end{bmatrix} = \begin{bmatrix} 1 \\ x_1 - 1 \\ 1 + x_3/2 \\ 1 + x_2/2 \\ -1 + x_3/2 \\ -1 + x_2/2 \end{bmatrix} \quad (26)$$

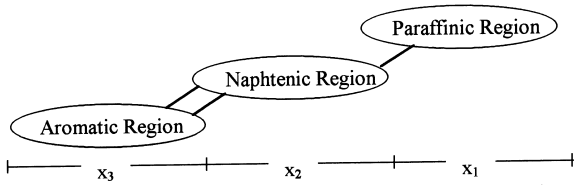

Fig. 4. Connectivity among sub-structures of a typical molecule.

where the superscript ($^{\text{r}}$) indicates ring increments. Once again, summations are performed as in Eqs. (22)–(24) with Eq. (26) and the values in Table 2.

4. Flash at fixed T and P

We begin VLE analysis by the flash calculation with T and P fixed. Balance equations, equilibrium relations and normalization restrictions are similar to the ones used for discrete mixtures. The main differences are as follows:

1. It is a functional-algebraic problem, because DFs are unknowns instead of the molar fractions of the discrete case;
2. The traditional summations over the species become integrals over the continuum spectrum of species.

The DFs of feed, vapor phase and liquid phase will be denoted by $f(\underline{x})$, $v(\underline{x})$ and $l(x)$, respectively. Rachford–Rice equation for flash calculation [15] takes a modified form, which is

$$\Phi_{\text{F}}(\beta) = \int_0^\infty \cdots \int_0^\infty \frac{f(\underline{x})[K(\underline{x}, P, T) - 1]}{\beta K(\underline{x}, P, T) + (1 - \beta)} \text{d}^n x = 0 \quad (27)$$

Its deduction is analogous to the discrete case, and uses a normalization condition with the form of Eq. (1). The DFs of vapor and liquid phases are then given by

$$l(\underline{x}) = \frac{f(\underline{x})}{\beta K(\underline{x}, P, T) + (1 - \beta)} \quad (28)$$

$$v(\underline{x}) = \frac{f(\underline{x}) K(\underline{x}, P, T)}{\beta K(\underline{x}, P, T) + (1 - \beta)} \quad (29)$$

where vaporization equilibrium ratio is calculated with

$$K(\underline{x}, P, T) = \frac{v(\underline{x})}{l(\underline{x})} = \frac{\phi^L(\underline{x}, P, T)}{\phi^V(\underline{x}, P, T)} \quad (30)$$

and vapor fraction is given by

$$\beta = \frac{V}{F} \quad (31)$$

It must be noticed that the dependence of the DFs on T and P was omitted for notation simplicity.

4.1. Simulations

Once the complete procedure is established, one can conduct simulations of the model. These simulations are carried out with the Quadrature Method as described in Cotterman and Prausnitz [7]. It is an interesting method based on the fact that only integrals of the DFs are needed for VLE calculation. Therefore, the system of Eqs. (27)–(31) becomes algebraic, once DFs must be evaluated only on quadrature points. An interpolation procedure can be used if information on DFs must be recovered between contiguous points.

For this method, Laguerre quadrature was used, which is based on the orthogonality of Laguerre polynomials over the

interval $(0,\infty)$. Quadrature points (xq_i) are the nq roots of the Laguerre polynomial of degree nq:

$$L_{nq}(x) = \sum_{k=0}^{nq}(-1)^{k+nq}\left[\frac{nq!}{(nq-k)!}\right]^2\frac{x^{nq-k}}{k!} \quad (32)$$

Quadrature weights (wq_i) are given by

$$wq_i = \left[\frac{nq!}{L_{nq+1}(xq_i)}\right]^2 xq_i\exp(xq_i) \quad (33)$$

A generic successive substitution algorithm can then be written:

1. Input variables: T, P, EOS parameters, and nq;
2. Input or statistical fitting of feed DFs' parameters;
3. Calculation of quadrature points and weights: wq_i and xq_i;
4. Set i=0;
5. Estimation of $f^q = f(\underline{x})$ and $K_i^q = (P^{\text{sat}}(\underline{x}, T))/P$ on quadrature points;
6. Calculation of β with $\Phi_F(\beta)$=0;
7. Calculation of $l_i^q = f^q/(\beta K_i^q + (1-\beta))$ and $v_i^q = f^q K_i^q/(\beta K_i^q + (1-\beta))$ on quadrature points;
8. Calculation of $K_{i+1}^q(\underline{x}) = (\phi^L(\underline{x}, P, T))/(\phi^V(\underline{x}, P, T))$ on quadrature points;
9. $K_{i+1}^q = K_i^q$?
   If not, make $K_i^q = K_{i+1}^q$, i=i+1 and go to (6).
10. Print graphical and numerical results.

Examples can be found in the literature [16,17] for the mentioned statistical fittings using experimental data for real mixtures, as though for typical experimental characterization. Such fittings are important and involve, basically, an integration of the DFs to produce 'lumped' information which can than be compared with experimental data. However, this procedure is also beyond the scope of this work, which concerns, mainly, the formulation and resolution of VLE of multi-indexed continuous mixtures.

So simulations will be conducted considering the already mentioned cases with arbitrarily chosen parameters for the feed DFs.

4.2. Case 1

It is the simplest case, and related integrals are calculated as internal products of two vectors, which makes computational routines very fast:

$$\int_0^\infty g(x)\mathrm{d}x \cong \sum_{i=1}^{nq} wq_i\, g(xq_i) \quad (34)$$

Conditions employed were η=10, ε=1, T=450 K and P=1 bar, and β was found to be 0.4958. The following figures, Figs. 5 and 6, were also obtained.

In Fig. 5, each line corresponds to an iteration on the outer loop of the algorithm (iteration on K_i^q); the spots are iterations on Eq. (27) on a given line. In Fig. 6, the results

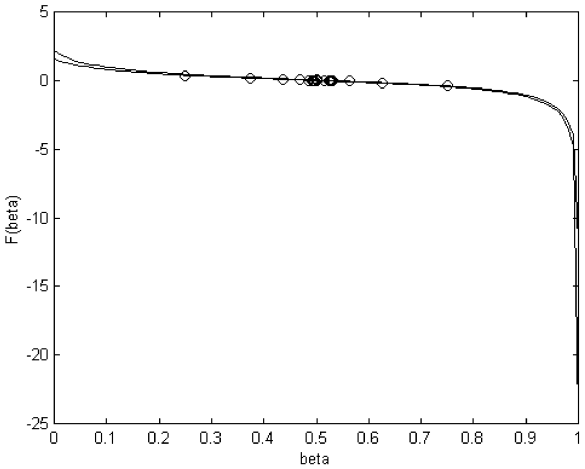

Fig. 5. Rachford–Rice equation solution (Case 1, η=10, ε=1, T=450 K and P=1 bar).

are shown in terms of quadrature points; if a smoother graph is needed, an interpolant DF can be fitted.

As can be noticed in Fig. 6, in liquid phase, the amount of heavy compounds is increased, and lighter species are preferably present in vapor, which is physically consistent. It must be pointed out that 18 quadrature points were used and errors on integrals were about 0.03%.

4.3. Case 2

This example has an interesting pictorial representation. Typical integrals can be calculated as quadratic forms, which is still computationally efficient:

$$\int_0^\infty\int_0^\infty g(x,y)\mathrm{d}x\,\mathrm{d}y \cong \sum_{j=1}^{nq^y}\sum_{i=1}^{nq^x} wq_j^y\, wq_i^x\, g(xq_i^x, xq_j^y) \quad (35)$$

Results for η_1=η_2=5, ε_1=ε_2=1, T=650 K and P=1 bar were β=0.6168 and the ones presented in Figs. 7–13.

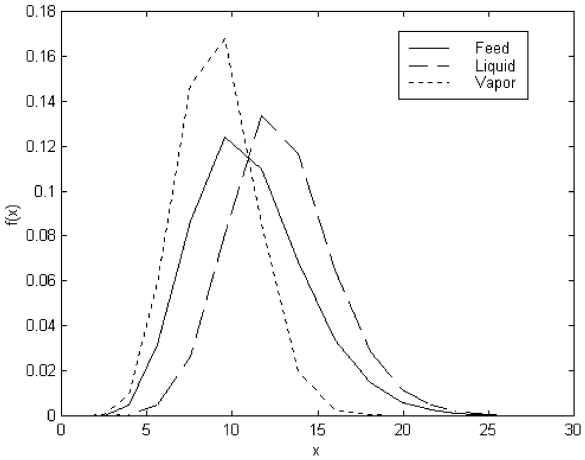

Fig. 6. DFs of feed, vapor phase and liquid phase (Case 1, η=10, ε=1, T=450 K and P=1 bar).

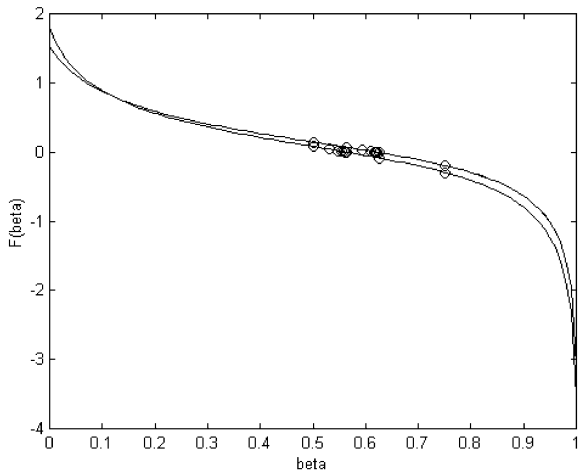

Fig. 7. Rachford–Rice equation solution (Case 1, $\eta_1=\eta_2=5$, $\varepsilon_1=\varepsilon_2=1$, $T=650$ K and $P=1$ bar).

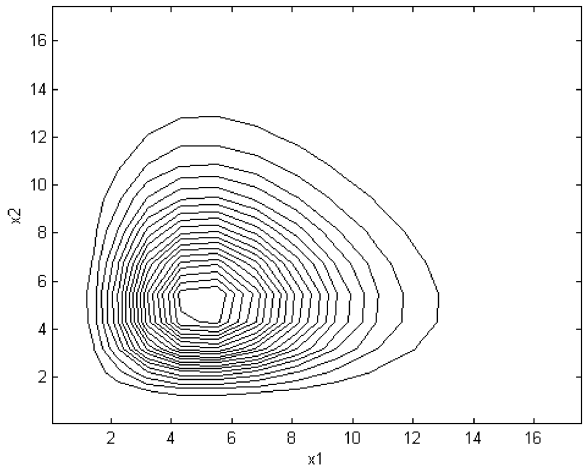

Fig. 8. Feed DF contours (Case 2, $\eta_1=\eta_2=5$, $\varepsilon_1=\varepsilon_2=1$, $T=650$ K and $P=1$ bar).

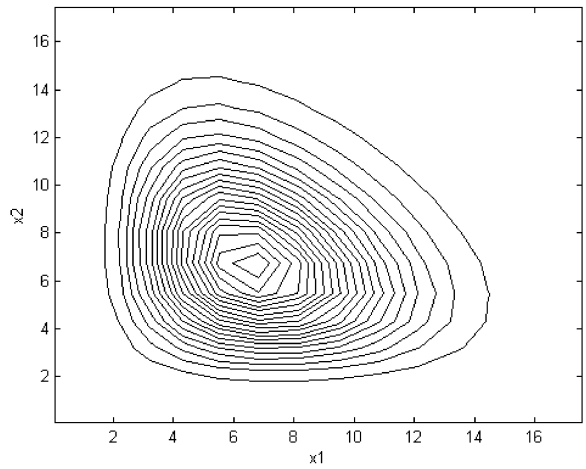

Fig. 9. Liquid DF contours (Case 2, $\eta_1=\eta_2=5$, $\varepsilon_1=\varepsilon_2=1$, $T=650$ K and $P=1$ bar).

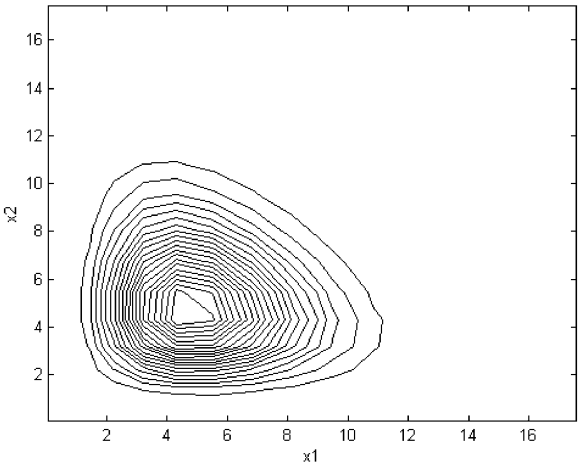

Fig. 10. Vapor DF contours (Case 2, $\eta_1=\eta_2=5$, $\varepsilon_1=\varepsilon_2=1$, $T=650$ K and $P=1$ bar).

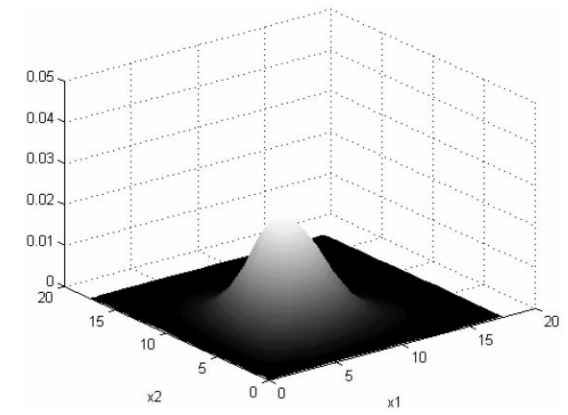

Fig. 11. Feed DF (Case 2, $\eta_1=\eta_2=5$, $\varepsilon_1=\varepsilon_2=1$, $T=650$ K and $P=1$ bar).

Once again, in Figs. 8–10, the results are shown in terms of quadrature points; if a smoother graph is needed, a 2-D interpolant DF can be fitted. They are of particular interest since they contain some important information. One may notice that, once again, physical consistency was achieved,

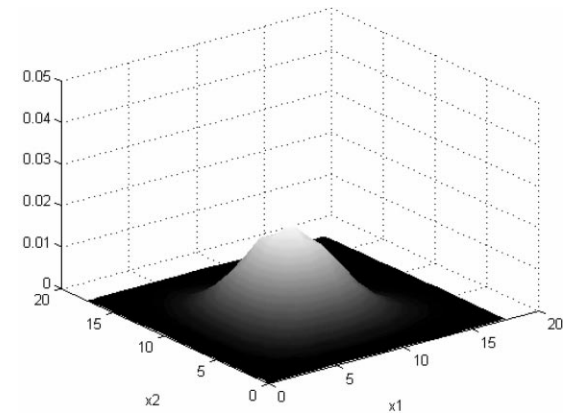

Fig. 12. Liquid DF (Case 2, $\eta_1=\eta_2=5$, $\varepsilon_1=\varepsilon_2=1$, $T=650$ K and $P=1$ bar).

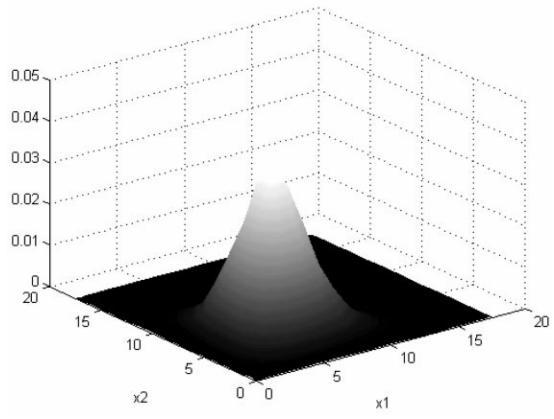

Fig. 13. Vapor DF (Case 2, $\eta_1=\eta_2=5$, $\varepsilon_1=\varepsilon_2=1$, $T=650$ K and $P=1$ bar).

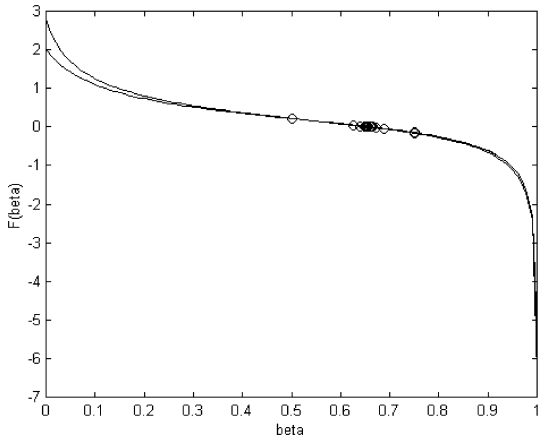

Fig. 14. Rachford–Rice equation solution (Case 3, $\eta_1=\eta_2=\eta_3=5$, $\varepsilon_1=\varepsilon_2=\varepsilon_3=1$, $T=675$ K and $P=1$ bar).

with heavier molecules migrating to liquid phase and lighter ones to vapor phase. However, the effect of one index on VLE is different from the other's, which can be seen through the distortion of liquid DF towards the x_1 direction. In fact, a carbon atom present in one portion of the molecule will not affect the molecule volatility the same way it would if it was to be in the other portion. It also must be said that this phenomenon can be stronger (and useful for separation techniques) in some particular mixtures.

This time, 20 quadrature points were used, leading to even smaller errors being observed on the values of the integrals.

4.4. Case 3

The three-indexed nature of this case introduces some difficulties and limitations. The calculation of the integrals related to this case involves at least one iterative loop, which considerably increases computational time:

$$\int_0^\infty \int_0^\infty \int_0^\infty g(x, y, z)\mathrm{d}x\,\mathrm{d}y\,\mathrm{d}z \cong \sum_{l=1}^{nq^z}\sum_{j=1}^{nq^y}\sum_{i=1}^{nq^x} wq_l^z\, wq_j^y\, wq_i^x\, g(xq_i^x, xq_j^y, xq_l^z) \quad (36)$$

The pictorial representation is limited by the fact that four coordinates would be necessary: three indices and the value of the DF itself. The solution was to create a gray scale in which the DF value is directly proportional to the intensity of the black color. Therefore, if the point (x_1, x_2, x_3) is marked with a black spot, it means that the molecule characterized by an index-vector (x_1, x_2, x_3) is the most frequently present in that mixture. The absence (or trace concentrations) of species is characterized by light gray spots.

Temperature and pressure employed were $T=675$ K and $P=1$ bar, feed DF parameters were $\eta_1=\eta_2=\eta_3=5$, $\varepsilon_1=\varepsilon_2=\varepsilon_3=1$, and the results were $\beta=0.6734$ and the ones depicted in Figs. 14–17.

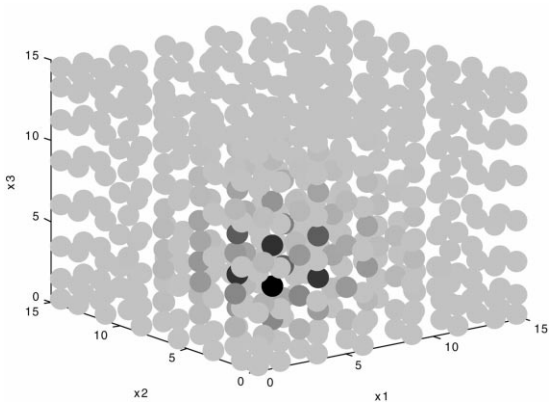

Fig. 15. Feed DF (Case 3, $\eta_1=\eta_2=\eta_3=5$, $\varepsilon_1=\varepsilon_2=\varepsilon_3=1$, $T=675$ K and $P=1$ bar).

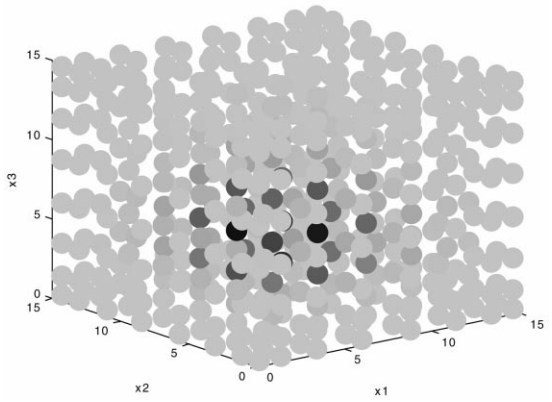

Fig. 16. Feed DF (Case 3, $\eta_1=\eta_2=\eta_3=5$, $\varepsilon_1=\varepsilon_2=\varepsilon_3=1$, $T=675$ K and $P=1$ bar).

Remarks on physical consistency are the same as in the previous case. Quadrature was still able to integrate DFs with small errors because 20 points were used, but CPU time increased within three orders of magnitude.

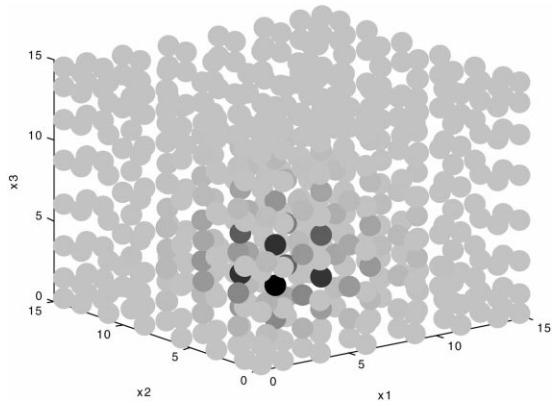

Fig. 17. Feed DF (Case 3, $\eta_1=\eta_2=\eta_3=5$, $\varepsilon_1=\varepsilon_2=\varepsilon_3=1$, $T=675$ K and $P=1$ bar).

5. Bubble and dew point calculation

Dew point and bubble point calculation are important tasks (for instance, when designing distillation columns) and Rachford–Rice equation, Eq. (27), can be used for this purpose. For dew point calculation, it is obvious that

$$\beta = 1 \tag{37}$$

$$v(\underline{x}) = f(\underline{x}) \tag{38}$$

and Eq. (27) becomes

$$\Phi_{\mathrm{D}}(T \text{ or } P)=\ln\left[\int_0^{\infty}\cdots\int_0^{\infty}\frac{f(\underline{x})}{K(\underline{x},P,T)}\mathrm{d}^n x\right]=0 \tag{39}$$

to be solved for T or P.

The logarithmic form of Eq. (39) is known to increase the convergence speed of numerical algorithms used to solve it. For bubble point calculation

$$\beta = 0 \tag{40}$$

$$l(\underline{x}) = f(\underline{x}) \tag{41}$$

and Eq. (27) becomes

$$\Phi_{\mathrm{B}}(T \text{ or } P) = \ln\left[\int_0^{\infty}\cdots\int_0^{\infty} f(\underline{x})K(\underline{x},P,T)\mathrm{d}^n x\right] = 0 \tag{42}$$

where T or P must be found.

5.1. Simulations

Once again, the quadrature method described in Section 4 will be employed. For these cases, the following generic successive substitution algorithm can then be written:

1. Input variables: P or T, EOS parameters, and nq;
2. Input or statistical fitting of feed DFs' parameters;
3. Calculation of quadrature points and weights: wq_i and xq_i;
4. Set $i=0$;
5. Estimation of $f^q = f(\underline{x})$ and $K_i^q = (P^{\mathrm{sat}}(\underline{x}, T))/P$ on quadrature points;
6. If dew point: $v^q = f^q$ and $l^q = v^q/K_i^q$
   If bubble point: $l^q = f^q$ and $v^q = K_i^q l^q$;
7. If dew point: calculate T or P with $\Phi_{\mathrm{D}}(T \text{ or } P)=0$, making $i=i+1$ and recalculating K_i^q and $l^q = v^q/K_i^q$ at each iteration
   If bubble point: calculate T or P with $\Phi_{\mathrm{B}}(T \text{ or } P)=0$, making $i=i+1$ and recalculating K_i^q and $v^q = K_i^q l^q$ at each iteration;
8. Print graphical and numerical results.

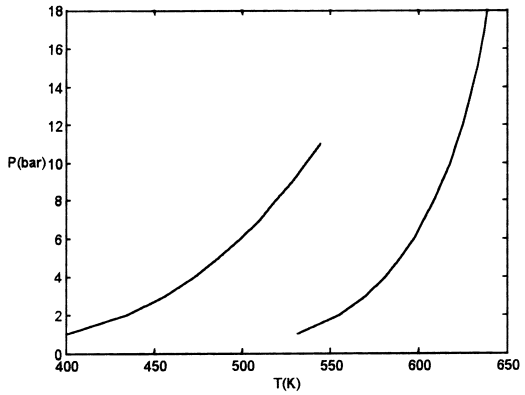

Fig. 18. Phase envelope (bubble and dew point loci) — Case 1.

5.1.1. Case 1

Graphical representations of phase envelopes are depicted as follows. It can be seen that there is a lack of closure. That is so because of the well known problem of convergence near critical points, whose treatment is beyond the scope of the present work (Fig. 18).

5.1.2. Case 2

In this system, closure problem is even worse (especially in the bubble curve) and must be intensively investigated if near critical point calculations have to be performed (Fig. 19).

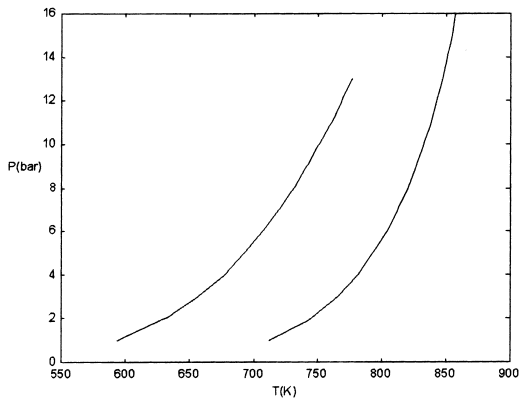

Fig. 19. Phase envelope (bubble and dew point loci) — Case 2.

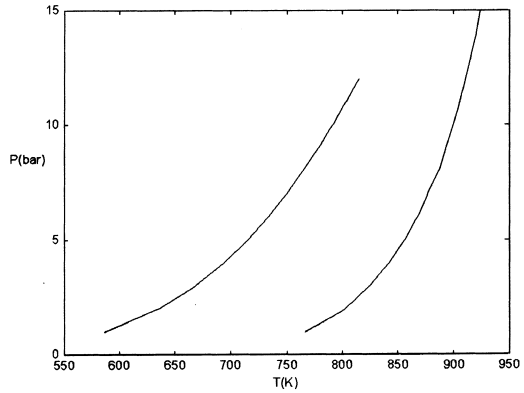

Fig. 20. Phase envelope (bubble and dew point loci) — Case 3.

5.1.3. Case 3

In this example, the closure problem is added to an excessively large computational time and special strategies must be developed (Fig. 20).

6. Conclusions and remarks

In this work, we described the vapor–liquid equilibrium of multi-indexed continuous mixtures, using the Peng–Robinson equation of state and Joback's group contribution method.

In previous works, mixtures that would be obviously characterized by an *n*-dimensional index have been commonly approximated as *n* families of species [18]. In this work, the multi-functional nature of molecules was respected with the usage of multi-dimensional indices.

In continuous mixtures context, EOS parameters have been traditionally addressed through fitted polynomials instead of their natural formulation, which is related to critical coordinates. So an adequate continuous index was chosen (the number of molecular groups), which made it possible to predict these coordinates easily, through Joback's method. For VLE calculations, a quadrature method was chosen, which turns the functional-algebraic system into an algebraic one. For that, two algorithms were presented.

Results were physically consistent since the amount of heavy species in the liquid phase increased and the vapor phase showed the expected increase in lighter species. It must be said that this effect was not equally distributed among the indices.

7. Nomenclature

a', B	entities defined by Eqs. (12) and (13)
a, b, m	P-R EOS parameter
$f(\underline{x})$, $v(\underline{x})$, $l(\underline{x})$	DFs
$J(\underline{x})$	Joback vector
$K(x,P,T)$	vaporization equilibrium ratio
$L_{nq}(x)$, nq, xq, wq	Laguerre quadrature parameters
P	pressure
P^{sat}	saturation pressure
R	universal gas constant
T	temperature
$T_{\text{b}}(\underline{x})$	normal boiling temperature
T_{c}, P_{c}	critical coordinates
v	molar volume
$\omega(\underline{x})$	acentric factor
$\underline{x}$	continuous index
z	compressibility factor

Greek letters

β	vapor fraction
ε, η	parameters of gamma DF

References

[1] J.C. Chachamovitz, M.Sc. Thesis (in Portuguese), Federal University of Rio de Janeiro, Brazil, 1993.
[2] R. Aris, G.R. Gavalas, Philos. Trans. R. Soc. A260 (1966) 351.
[3] J.A. Gualtieri, J.M. Kincaid, G. Morrison, J. Chem. Phys. 77 (1982) 521.
[4] J.J. Salacuse, G. Stell, J. Chem. Phys. 77 (1982) 3714.
[5] M.T. Rätzch, H. Kehlen, Fluid Phase Equilibria 51 (1989) 133.
[6] P.C. Du, G.A. Mansoori, Fluid Phase Equilibria 30 (1986) 57.
[7] R.L. Cotterman, J.M. Prausnitz, Ind. Eng. Chem. Proc. Des. Dev. 24 (1985) 434.
[8] J.G. Briano, E.D. Glandt, Fluid Phase Equilibria 14 (1983) 91.
[9] R.L. Cotterman, R. Bender, J.M. Prausnitz, Ind. Eng. Chem. Proc. Des. Dev. 24 (1985) 194.
[10] B.T. Willman, A.S. Teja, AIChE J. 32 (1986) 2067.
[11] D.Y. Peng, D.B. Robinson, Ind. Eng. Chem. Fundam. 15 (1976) 59.
[12] G.L. Rochocz, M.Sc. Thesis (in Portuguese), Federal University of Rio de Janeiro, Brazil, 1990.
[13] K.G. Joback, SM. Thesis in Chemical Engineering, Massachusetts Institute of Technology, MA, 1984.
[14] R.J. Quann, S.B. Jaffe, Chem. Eng. Sci. 51 (1996) 1615.
[15] H.H. Rachford, J.D. Rice, Petrol. Technol. Sect. 1 (1952) 19.
[16] F.C. Peixoto, J.L. de Medeiros, Braz. J. Chem. Eng. 3 (1999) 229.
[17] F.C. Peixoto, J.L. de Medeiros, Braz. J. Chem. Eng. 1 (1999) 65.
[18] M. Sportisse, A. Barreau, P. Ungerer, Fluid Phase Equilibria 139 (1997) 255.